ground water

Propagation of Seasonal Temperature Signals into an Aquifer upon Bank Infiltration

by Nelson Molina-Giraldo[1], Peter Bayer[2], Philipp Blum[3], and Olaf A. Cirpka[4]

Abstract

Infiltrating river water carries the temperature signal of the river into the adjacent aquifer. While the diurnal temperature fluctuations are strongly dampened, the seasonal fluctuations are much less attenuated and can be followed into the aquifer over longer distances. In one-dimensional model with uniform properties, this signal is propagated with a retarded velocity, and its amplitude decreases exponentially with distance. Therefore, time shifts in seasonal temperature signals between rivers and groundwater observation points may be used to estimate infiltration rates and near-river groundwater velocities. As demonstrated in this study, however, the interpretation is nonunique under realistic conditions. We analyze a synthetic test case of a two-dimensional cross section perpendicular to a losing stream, accounting for multi-dimensional flow due to a partially penetrating channel, convective-conductive heat transport within the aquifer, and heat exchange with the underlying aquitard and the land surface. We compare different conceptual simplifications of the domain in order to elaborate on the importance of different system elements. We find that temperature propagation within the shallow aquifer can be highly influenced by conduction through the unsaturated zone and into the underlying aquitard. In contrast, regional groundwater recharge has no major effect on the simulated results. In our setup, multi-dimensionality of the flow field is important only close to the river. We conclude that over-simplistic analytical models can introduce substantial errors if vertical heat exchange at the aquifer boundaries is not accounted for. This has to be considered when using seasonal temperature fluctuations as a natural tracer for bank infiltration.

Introduction

A surface-water body that infiltrates into an aquifer also influences the subsurface temperature regime. Temporal fluctuations of temperature have been recognized as a natural tracer that may be used for hydrogeological interpretation (Suzuki 1960; Stallman 1965; Lapham 1989; Constantz 1998; Conant 2004; Anderson 2005; Blasch et al. 2006; Hatch et al. 2006; Hoehn and Cirpka 2006; Keery et al. 2007; Duque et al. 2010; Vogt et al. 2010, among others). Natural temperature variations are attractive tracers, because they are intrinsic to the system. In contrast to synthetic tracers in well-to-well or river-to-well applications, no additional injection campaigns are necessary, thus avoiding alterations of the natural flow regime and groundwater chemistry (Constantz et al. 2003). Furthermore, none of the regulative constraints that may apply for conventional tracers, such as fluorescent dyes, have to be considered. Finally, groundwater temperature can easily be measured over long time periods in monitoring wells by means of relatively inexpensive thermometers, commonly included in water-level loggers (Stonestrom and Blasch 2003; Anderson 2005; Ma and Zheng 2010).

[1]Corresponding author: Center for Applied Geoscience (ZAG), University of Tübingen, Sigwartstraße 10, 72076 Tübingen, Germany; (49) 7071 2973172; fax: (49) 7071 295059; nelson.molina-giraldo@uni-tuebingen.de

[2]Engineering Geology, ETH Zürich, Sonneggstraße 5, 8092 Zurich, Switzerland.

[3]Institute for Applied Geosciences (AGW), Karlsruhe Institute of Technology (KIT), Kaiserstraße 12, 76131 Karlsruhe, Germany.

[4]Center for Applied Geoscience (ZAG), University of Tübingen, Sigwartstraße 10, 72076 Tübingen, Germany.

Received March 2010, accepted July 2010.

doi: 10.1111/j.1745-6584.2010.00745.x

Variation of radiation and air temperature causes fluctuation of surface-water temperatures. Typically, the most pronounced signals are related to diurnal and seasonal changes of short-wave radiation triggered by the path of the sun. These periodic signals are superimposed by variations on the time scale of several days caused by synoptic weather phenomena. The temperature signals are transmitted from the surface-water body into a connected aquifer by conduction and convection. The latter denotes heat transport by the moving water. Mixing processes due to microscale differential groundwater velocity and macroscale geological heterogeneities create thermal dispersion (Bear 1972). Heat transfer by conduction is governed by the temperature gradient. Accordingly, the dominant processes are convection at high infiltration rates, and conduction in parts of the subsurface with slowly flowing or even stagnant water.

As the temperature signal penetrates into the aquifer, it is dampened (i.e., the amplitude is attenuated) and shifted in time. As an illustrative example, Figure 1 shows the temperature time series measured in the losing River Thur, Switzerland, and an observation well at about 50 m distance. Details of the corresponding field study are described by Cirpka et al. (2007). The river time series exhibits a seasonal trend, which can be approximated well by a sinusoidal function with amplitude of about 8 K. The river signal also includes diurnal variations (amplitude of about 2 K in the summer), which are graphically not well resolved in Figure 1. Apparently, the groundwater time series of the observation well has lost the diurnal signal, whereas the seasonal variation is hardly dampened and slightly shifted toward later times. Hence, after some travel distance the remaining temperature signal is the seasonal one.

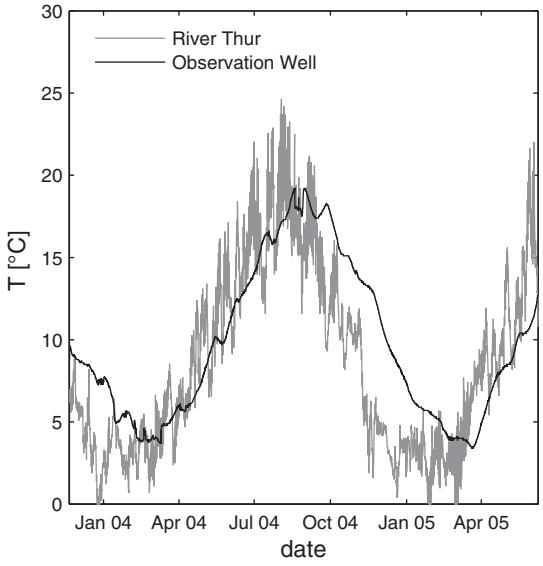

Figure 1. Temperature time series of 2004 to 2005 measured in the River Thur, Switzerland, and in an adjacent groundwater observation well in 50 m distance to the river (Cirpka et al. 2007).

The time series of Figure 1 are representative for losing rivers and associated alluvial aquifers in middle latitudes, with considerable annual temperature variations and substantial infiltration. The degree of dampening depends on the groundwater flow velocity, the thermal diffusivity, and the frequency of the temperature signal (Stallman 1965). High-frequency (e.g., diurnal) temperature fluctuations are more dampened than low-frequency (e.g., seasonal) ones, because the related spatial temperature profiles have larger gradients, even with identical amplitudes. Typically, diurnal temperature signals become undetectable at infiltration distances that are considerably larger than 1 m. In recent years, the analysis of these signals in vertical profiles within river beds has been used in various studies to estimate local exchange rates of water in both losing and gaining streams (Hatch et al. 2006; Keery et al. 2007; Constantz 2008; Vogt et al. 2010). The method requires measurement equipment to be installed within the river on a mostly temporary basis, because it would not withstand mechanical stresses during floods.

In contrast to diurnal fluctuations, seasonal temperature signals may penetrate to distances of tens to hundreds of meters and can therefore be detected in standard piezometers equipped with thermometers in the vicinity of the river, like in the case depicted in Figure 1. In theory, seasonal temperature fluctuation might therefore be used to infer residence times of water and flow rates in alluvial aquifers, which are required for planning of freshwater extraction wells close to rivers. However, Hoehn and Cirpka (2006) warned that the interpretation of seasonal temperature variations as natural tracers for bank infiltration may be impeded by interference with seasonal temperature signals from sources other than the infiltrating river water. They were mainly arguing that several water streams of shallow origin may mix within the subsurface.

The objective of this study is to examine in detail how the seasonal temperature signal of a river is propagated into an adjacent aquifer. In particular, we want to elucidate to what extent a unique interpretation from measurements in individual groundwater observation wells is possible. A synthetic case is defined with a river that continuously infiltrates into an aquifer with an overlying unsaturated zone and an underlying aquitard. The setup is based on a typical alluvial aquifer with shallow water table and small aquifer thickness (Hoehn and Cirpka 2006; Riva et al. 2006). Simulations are performed for an idealized vertical cross section in the general groundwater flow direction. While applications of numerical models for temperature transport in aquifers influenced by surface-water bodies have been presented in several studies (Lapham 1989; Bundschuh 1993; Ronan et al. 1998; Bravo et al. 2002; Constantz et al. 2002; Niswonger and Prudic 2003; Bense and Kooi 2004; Su et al. 2004; Blasch et al. 2006; Barlow and Coupe 2009; Duque et al. 2010), the purpose of the current work is to analyze how conceptual simplifications of the surface and subsurface, such as recharge, multi-dimensionality of the flow field due to a partially

penetrating channel, and conduction into the aquitard and the top layer, impact the accuracy of the simulations of temperature fluctuations.

Mathematical Model

Governing Equations

In the synthetic case study, we consider steady-state groundwater flow without internal sources and sinks following the standard groundwater flow equation (Bear 1972; de Marsily 1986):

$$\nabla \cdot (K \nabla h) = 0 \tag{1}$$

subject to the following boundary conditions:

$$h = \hat{h} \text{ on } \Gamma_1 \tag{2}$$

$$(K \nabla h) \cdot \boldsymbol{n} = \hat{q} \text{ on } \Gamma_2 \tag{3}$$

where h denotes the hydraulic head and K is the hydraulic conductivity assumed isotropic; $\hat{h}$ and $\hat{q}$ are prescribed values of the hydraulic head at boundary Γ_1 and the normal inwardly directed flux at boundary Γ_2, respectively; $\boldsymbol{n}$ is the unit normal vector pointing outward. For the unsaturated zone, the effective saturation and unsaturated hydraulic conductivity are computed using the van Genuchten-Mualem parameterization (van Genuchten 1980):

$$S_e(h_c) = \left(1 + (\alpha h_c)^N\right)^{(1-N)/N} \tag{4}$$

$$K(h_c) = K_{sat} \sqrt{S_e} \left(1 - \left(1 - S_e^{N/(N-1)}\right)^{(N-1)/N}\right)^2 \tag{5}$$

where S_e denotes the effective water saturation, α and N are the van Genuchten parameters depending on the soil type, and K_{sat} is the saturated hydraulic conductivity. The capillary head (h_c) is calculated as follows:

$$h_c = \min(z - h, 0) \tag{6}$$

where z is the elevation above a reference datum and h is the hydraulic head referenced to the same datum.

Heat transport in porous media is expressed by the convection-dispersion equation, written here in a form that is formally identical to the advection-dispersion equation for solute transport (de Marsily 1986; Domenico and Schwartz 1998):

$$\frac{\partial T}{\partial t} + \nabla \cdot (\mathbf{v}_T T) - \nabla \cdot (\mathbf{D} \nabla T) = 0 \tag{7}$$

where T denotes temperature, t is time, $\mathbf{v}_T$ is the effective velocity of convective heat transport, and $\mathbf{D}$ is the dispersion tensor for conductive-dispersive heat transfer. For heat transfer, the boundary Γ of the domain is subdivided into the inflow section Γ_{in} and a fixed-temperature section Γ_{fix}, both at which we assume a known temperature value, and the remaining part $\Gamma/(\Gamma_{in} \cup \Gamma_{fix})$ across which the conductive-dispersive heat transport is set to be zero:

$$T = \hat{T}_0(t) \qquad \text{on } \Gamma_{in} \cup \Gamma_{fix} \tag{8}$$

$$(\mathbf{D} \nabla T) \cdot \boldsymbol{n} = 0 \qquad \text{on } \frac{\Gamma}{\Gamma_{in} \cup \Gamma_{fix}} \tag{9}$$

where $\hat{T}_0(t)$ is the temperature at $\Gamma_{in} \cup \Gamma_{fix}$. In our application, $\hat{T}_0(t)$ varies periodically in time.

The temperature dispersion tensor $\mathbf{D}$ is parameterized as follows (Bear 1972):

$$\mathbf{D}_{ij} = \frac{v_{Ti} v_{Tj}}{\|\mathbf{v}_T\|}(\alpha_l - \alpha_t) + \delta_{ij}\left(\frac{\lambda_m}{\rho_m c_m} + \alpha_t \|\mathbf{v}_T\|\right) \tag{10}$$

where α_l and α_t are the longitudinal and transverse thermal dispersivities, respectively; λ_m is the thermal conductivity; $\rho_m c_m$ is the volumetric heat capacity of the porous medium; and δ_{ij} is the Kronecker delta function which is one for $i = j$ and zero otherwise.

The effective thermal velocity of convective heat transport $\mathbf{v}_T$ is related to specific discharge $\mathbf{q}$ and the seepage velocity of conservative solute transport $\mathbf{v}_a$ as follows:

$$\mathbf{v}_T = \frac{\mathbf{q} \rho_w c_w}{\rho_m c_m} = \mathbf{v}_a \frac{\theta \rho_w c_w}{\rho_m c_m} = \frac{\mathbf{v}_a}{R_T} \tag{11}$$

where $\rho_w c_w$ is the volumetric heat capacity of water and θ is the porosity. R_T denotes the ratio of seepage velocity to effective thermal velocity of heat transport, also known as retardation factor of temperature, which is given as the ratio between the volumetric heat capacities of the porous medium, $\rho_m c_m$ and water $\Theta_w \rho_w c_w$ in which Θ_w is the volumetric water content. The volumetric heat capacity of the bulk porous medium is computed as the weighted arithmetic mean of the solids ($\rho_s c_s$) and water ($\rho_w c_w$) (Domenico and Schwartz 1998; Anderson 2005). The contribution of the gas phase is ignored due to its low density:

$$\rho_m c_m = \Theta_w \rho_w c_w + (1 - \theta) \rho_s c_s \tag{12}$$

The volumetric water content (Θ_w) can be computed as follows (van Genuchten 1980):

$$\Theta_w = S_e(\Theta_s - \Theta_r) + \Theta_r \tag{13}$$

where Θ_r and Θ_s are the values of residual and saturated volumetric water content.

The weighted geometric mean of the thermal conductivity of the solids (λ_s), water (λ_w), and gas phase (λ_g) is used to calculate the thermal conductivity, λ_m, of the bulk porous media in the unsaturated zone (Nield and Bejan 2006):

$$\lambda_m = \lambda_s^{1-\theta} \lambda_w^{\Theta_w} \lambda_g^{\theta - \Theta_w} \tag{14}$$

Analytical Solution in One Spatial Dimension

If possible, it is desirable to use fast and straightforward analytical solutions. Most of the analytical approaches available to determine infiltration rates based on temperature measurements follow the works by Suzuki (1960), Stallman (1965), and Bredehoeft and Papaopulos (1965). Stallman (1965) extended the analytical solution given by Suzuki (1960) for computing infiltration and exfiltrating rates under transient conditions and periodic boundary conditions. Bredehoeft and Papaopulos (1965) presented a steady-state analytical solution for calculating vertical rates of groundwater movement. Taniguchi (1993), Goto et al. (2005), Hatch et al. (2006), and Keery et al. (2007), among others, used Stallman's (1965) analytical expression to calculate vertical groundwater fluxes based on periodic surface temperature fluctuations. All these one-dimensional (1D) analytical solutions are restricted to special conditions in which heat transfer between the periodic temperature boundary and the observation point can be approximated by strictly 1D convective-dispersive transport.

The Fourier transform (see Appendix) of Equation 7 in a 1D system with uniform properties reads as:

$$2\pi if\tilde{T} + \mathbf{v}_\mathrm{T}\frac{\partial \tilde{T}}{\partial x} - D\frac{\partial^2 \tilde{T}}{\partial x^2} = 0 \tag{15}$$

subject to the boundary conditions:

$$\tilde{T}(x = 0, t) = \tilde{T}_0(f) \tag{16}$$

$$\tilde{T}(x = \infty, t) = 0 \tag{17}$$

The solution for Equations 15 through 17 is an exponential function with complex argument:

$$\tilde{T}(x, f) = \tilde{T}_0(f)\ \exp(-\lambda x) \tag{18}$$

where λ denotes a complex decay coefficient:

$$\lambda(f) = \frac{\sqrt{\mathbf{v}_\mathrm{T}^2 + 8\pi ifD} - \mathbf{v}_\mathrm{T}}{2D} \tag{19}$$

Substituting Equation 18 into the back Fourier transform of Equation A1 yields:

$$T(x, t) = \int_{-\infty}^{\infty} \tilde{T}_0(f) \exp\left[-\lambda(f)x\right] \exp(2\pi ift)\mathrm{d}f \tag{20}$$

Splitting λ into its real (λ_R) and imaginary (λ_I) components, results in the following two equations:

$$T(x, t) = \int_{-\infty}^{\infty} \tilde{T}_0(f) \exp(-\lambda_\mathrm{R}x) \exp\left[2\pi if\left(t - \frac{x}{c}\right)\right]\mathrm{d}f \tag{21}$$

$$c = \frac{2\pi f}{\lambda_\mathrm{I}} \tag{22}$$

where c is the celerity of the sinusoidal wave propagation. Finally, considering the specific case of a sinusoidal temperature signal $T_0(t)$ with amplitude a_T and the phase shift φ,

$$T_0(t) = a_{\mathrm{T}\cos}(\varphi + 2\pi ft) \tag{23}$$

The solution in the time domain is as follows (Stallman 1965):

$$T(x, t) = a_\mathrm{T}\ \exp(-\lambda_\mathrm{R}x)\ \cos\left[\varphi + 2\pi f\left(t - \frac{x}{c}\right)\right] \tag{24}$$

Numerical Simulation in a Vertical Cross Section

In order to account for more complex processes and geometries than realized by standard analytical methods, numerical simulation is needed. In the present work, the finite element method is used to solve the governing equations in two spatial dimensions. A vertical cross section of an alluvial aquifer adjacent to a river is simulated in detail. The standard Galerkin method is used to simulate the groundwater flow equation (Equation 1) and the Streamline-Upwind Petrov-Galerkin method (Brooks and Hughes 1982) is applied to the heat-transport equations in the Fourier domain (Equations A6 and A7). A uniform grid of bilinear rectangular elements of constant coefficients discretizes the cross section. Each grid element has 0.1 m height and 1 m length. The model output is the spatial field of the Fourier-transformed temperature $\tilde{T}$, which is a complex number. The magnitude and the angle of the complex temperature represent the amplitude (a_T) and the phase shift (φ) of the periodic temperature signal:

$$a_\mathrm{T} = \|\tilde{T}\| \tag{25}$$

$$\varphi = \tan^{-1}\left|\frac{\mathrm{Re}(\tilde{T})}{\mathrm{Im}(\tilde{T})}\right| \tag{26}$$

Model Setup

The case study represents a straight river with vertical and lateral infiltration. Seven model variants of different complexity are set up to examine the role of different conceptual assumptions (Figure 2). They are used to simulate temperature changes in the aquifer due to infiltration and hence are all oriented perpendicular to the river. Note that for strongly meandering rivers and even for straight rivers with a component of groundwater flow parallel to the channel, the assumption of essentially two-dimensional (2D) flow might not be valid (Woessner 2000). We start with a full model (scenario 1) accounting for conductive/dispersive and convective heat transfer in the groundwater flow field, conductive heat transfer into an underlying aquitard, and an unsaturated zone on top. For the latter, heat parameters depend on the volumetric water content as denoted by Equations 12 and 14. The full model also simulates convective heat transfer by groundwater recharge, and seasonal fluctuations of the

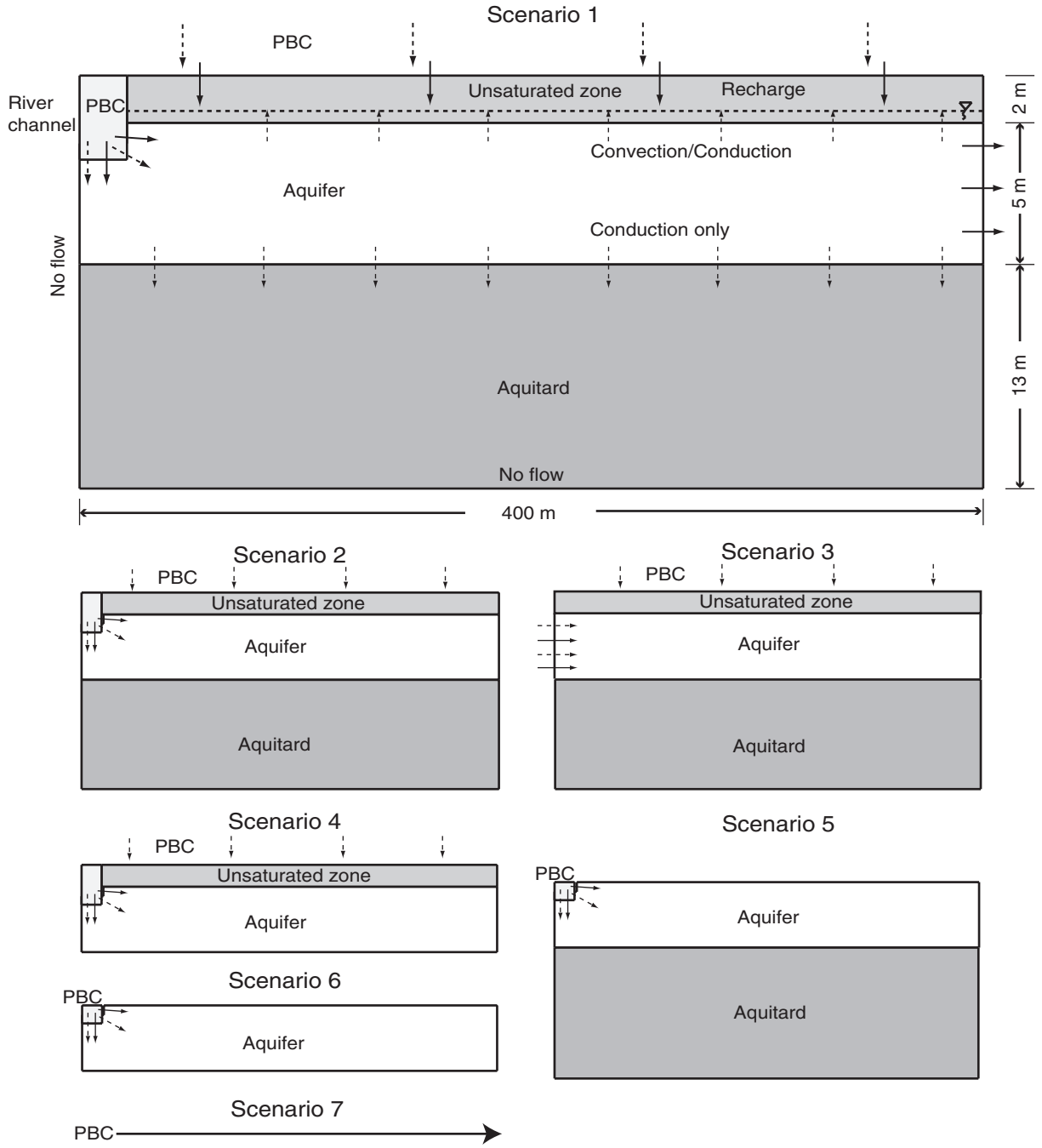

Figure 2. Model setups of different complexity. Scenarios 1 (full model), 2 (without recharge), 3 (fully penetrating channel), 4 (without aquitard), 5 (without unsaturated zone), 6 (only aquifer), and 7 (1D analytical solution). PBC: temperature periodic boundary conditions; dashed arrow: heat transfer (convection and conduction); solid arrow: water flow.

surface and river temperature. The geothermal heat flux is not considered because it is constant in time. Each of the listed processes adds additional complexity to the model and so the question is which components might be neglected while still arriving at valid temperature predictions in the aquifer. To answer this, the full model is simplified by eliminating groundwater recharge (scenario 2), multi-dimensionality of the flow field and hence assuming a fully penetrating channel (scenario 3), conduction in the aquitard (scenario 4), heat transfer in the top layer (scenario 5), and also a combination of the last two (scenario 6). The resultant six different model conceptualizations are numerically solved in 2D in the Fourier domain. The simplest model (scenario 7) is the representation of the aquifer as a 1D column connected to the river, which is simulated using the analytical expression by Stallman (1965) (Equation 24).

The full model (scenario 1) is considered the most accurate and thus serves as a reference to be compared with the other scenarios. As a criterion, the root mean square error (RMSE) is selected, which quantifies the residual error of the temperature evolution in the aquifer

between the full model and the simplified ones. The RMSE is applied to the complex temperature as follows:

$$\mathrm{RMSE} = \sqrt{\frac{1}{2A_{\mathrm{aq}}}\int_{A_{\mathrm{aq}}} \{\mathrm{Re}[T_1(x) - T_2(x)]\}^2 + \{\mathrm{Im}[T_1(x) - T_2(x)]\}^2 \mathrm{d}x} \quad (27)$$

where A_{aq} is the cross-sectional area of the aquifer within the model plane.

Similar boundary conditions to scenarios 1 and 2 were used by Bundschuh (1993) and Duque et al. (2010). The latter evaluated the surface water-groundwater interaction by a heat-tracer test using the heat-transport code VS2DHI (Healy and Ronan 1996). Bundschuh (1993) applied the USGS code SUTRA (Voss 1984) to evaluate the influence of the seasonal temperature fluctuations at the surface on the temperature of the aquifer.

Boundary Conditions and Aquifer Geometry

Scenario 1 (full model) is built of three horizontal layers (Figure 2). The upper layer (sandy loam) represents the unsaturated zone, the middle layer (sandy gravel) the aquifer, and the bottom layer (clay) the aquitard. Many alluvial aquifers exhibit a small distance to groundwater and a small aquifer thickness (Hoehn and Cirpka 2006; Riva et al. 2006). Accordingly, the thickness of the unsaturated zone is set to 2 m and that of the aquifer to 5 m. A thickness of 13 m is assigned to the aquitard to minimize boundary effects by the model bottom while including heat conduction into the aquitard. A preliminary analysis showed that for larger aquitard thicknesses the results do not change considerably. The horizontal length of the model domain is set to be 400 m. However, different lengths are also inspected in order to evaluate the effect of the scale of the model domain. No-flow boundary conditions are applied to the left and bottom boundary. Half of the river channel (10 m) is implemented at the upper left boundary. The other half of the river channel is assumed to be symmetrical.

A constant head in the river is assumed. The rationale for this assumption is that the fluctuations of the river stage and infiltration rates average out on the seasonal time scale considered here. This may be representative for rivers where the water level is regulated (e.g., by reservoirs), or for humid climates where water-level fluctuations of the river throughout the year are small. Accordingly, the presented approach may only yield approximate results for cases with strong variation of infiltration rates.

In the model, fixed-head boundary conditions are applied to the river and the right model face. The water enters the aquifer by infiltration through the river bed and the groundwater leaves the domain through the right boundary in the aquifer. A uniform regional recharge rate of 300 mm per year is allocated to the top boundary, which is a typical value of groundwater recharge in central Europe (Langguth and Voigt 2004). Fourier transformation in time is used to evaluate the periodic boundary conditions at the river and the top boundary. The temperature fluctuations are specified by an amplitude of 8 K and a frequency of 1/year.

Table 1
Hydraulic and Thermal Parameters Used in the Simulations (de Marsily 1986; Carsel and Parrish 1988; Spitz and Moreno 1996)

Specific heat capacity of solids (J/kg/K)	880
Specific heat capacity of water (J/kg/K)	4190
Density of the solids (kg/m^3)	2650
Thermal conductivity of solids (W/m/K)	2.00
Thermal conductivity of water (W/m/K)	0.58
Thermal conductivity of gas phase (W/m/K)	0.025
Total porosity (−)	0.30
Longitudinal dispersivity (m)	1.0
Transverse dispersivity (m)	0.01
Hydraulic gradient (‰)	3
Saturated hydraulic conductivity (m/s)	
Aquifer	1.0×10^{-3}
Aquitard	1.0×10^{-10}
Unsaturated zone	1.0×10^{-6}
van Genuchten parameters	
α (1/m)	3.6
N	1.56

Aquifer Parameters

Hydraulic and thermal aquifer parameters used in the simulation are typical for sandy aquifers. Values are listed in Table 1. Due to the low variability of thermal parameters compared with hydraulic parameters, the same values of the thermal conductivity and heat capacity are used for the three horizontal layers. The hydraulic conductivity values listed in Table 1 are for saturated sediments. The resulting groundwater velocity in the aquifer is almost equal to 1 m/day assuming a hydraulic gradient of 3‰. The aquifer system is assumed to be isotropic with respect to hydraulic conductivity. The effects of buoyancy and changes in viscosity are neglected. Therefore, the hydraulic and thermal parameters are assumed to be independent of the temperature changes. The effect of density and viscosity in heat-transport problems for shallow aquifers is discussed, for example, by Hecht-Méndez et al. (2010) and Ma and Zheng (2010). The latter stated that variable density and viscosity due to temperature changes of less than 15 K seem to be negligible in the flow model. In the present study, an atmospheric temperature change of 16 K is assumed between winter and summer. Nevertheless, at any given time, the temperature variability within the model domain is not larger than 10 K.

Results and Discussion

Full Model Simulations

Results for the full model (scenario 1) are obtained numerically in 2D in the Fourier domain. Figure 3 shows the calculated spatial distribution of the seasonal

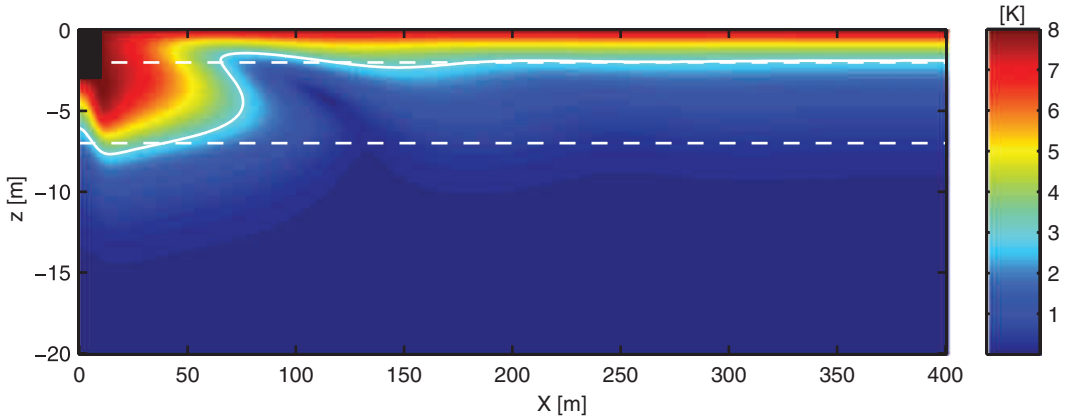

Figure 3. Simulated amplitude of the seasonal temperature signal for the full model (scenario 1). The river is located in the upper left corner. Dashed white lines: top and bottom of the aquifer; solid white line: penetration distance defined by an amplitude of $a_0 \times \exp(-1) \approx 2.94$ K.

temperature amplitude. The temperature signal originating from the river is propagated over the entire aquifer thickness close to the river and over a distance of approximately 90 m. Further away from the river, the signal originating from the surface is almost completely dampened in the unsaturated zone and in the first top meter of the aquifer. The degree of dampening of the temperature signals is linked to the groundwater flow velocity, the thermal diffusivity, and the frequency of the temperature signal. The penetration distance of the temperature signal is the distance at which the temperature amplitude in the subsurface has fallen to e^{-1} (i.e., 37%) compared to that of the periodic signal at the surface (Goto et al. 2005; Vogt et al. 2010). From Equation 24, the penetration distance (x_s) of the temperature front in a 1D system is therefore defined as $1/\lambda_R$, which can be expressed as follows:

$$x_s = \frac{2D}{\sqrt{(v_T^2/2) + \sqrt{(v_T^4/4) + 16\pi^2 f^2 D^2}} - v_T} \tag{28}$$

In case of zero convection Equation 28 simplifies to:

$$x_s(v_T = 0) = \sqrt{\frac{D}{\pi f}} \tag{29}$$

Assuming the unsaturated zone as a 1D problem in the vertical direction, the computed penetration depth in the unsaturated zone for the full model is about 2 m for seasonal fluctuations. In contrast, for diurnal fluctuations the vertical temperature signal is almost completely dampened in the first 0.20 m. We can conclude that although the seasonal temperature signal originating from the surface is strongly dampened through the unsaturated zone, it could still have an effect on the aquifer temperature depending on the thickness of the unsaturated zone.

Figure 4 shows the time shift or apparent travel time of temperature. The time shift in Figure 4a is plotted based on the wrapped phase shift. Therefore, the time shift is restricted to cycles of 1 year. In comparison, Figure 4b presents the results after correcting the phase shift by adding multiples of 2π in order to obtain a continuous function (unwrapped time shift) of apparent travel times of temperature.

Evidently, Figure 4a can result in misinterpretations of the apparent travel times of temperature due to the wrapped phase shift. A mismatch by multiples of 1 year can occur depending on the point of view the time shift profile is observed. Consider the following example: A hypothetical observation well is located 200 m away from the river and two measuring points of groundwater temperature are placed at 3 m (OW-d1) and 5 m (OW-d2) depth (Figure 4). The time shift observed at the 5 m depth point can be either 120 or 485 days, depending on the interpretation. For a vertical profile starting at the ground surface, the travel time of temperature would be misinterpreted as 120 days. For a longitudinal profile starting at the left boundary of the model, the actual travel time of temperature is 485 days. At the 3 m depth point, an apparent temperature travel time of 85 days is identified. Assuming a retardation factor of 2.2, we get a residence time of water of 39 days, which is actually a measure of the signal originating mainly from the surface and not the river. Thus, interpretation of travel times based on seasonal signals originating from an infiltrating river might be affected by interference with additional sources of temperature fluctuations.

The black dot in Figure 4a marks a point where the interfering periodic signals originating from the river and from the surface cancel out, the amplitude is zero, and the time shift is not defined. It is intuitively clear that seasonal temperature time series observed at profiles downgradient of this point within the aquifer should not be interpreted by a simple 1D analytical model. Figure 4a, however, also exemplifies that upstream of that point a substantial vertical profile of apparent travel time can be observed, either due to multi-dimensionality of the flow field (close to the river) or due to interference with conduction into the top and bottom layers (further away from the river).

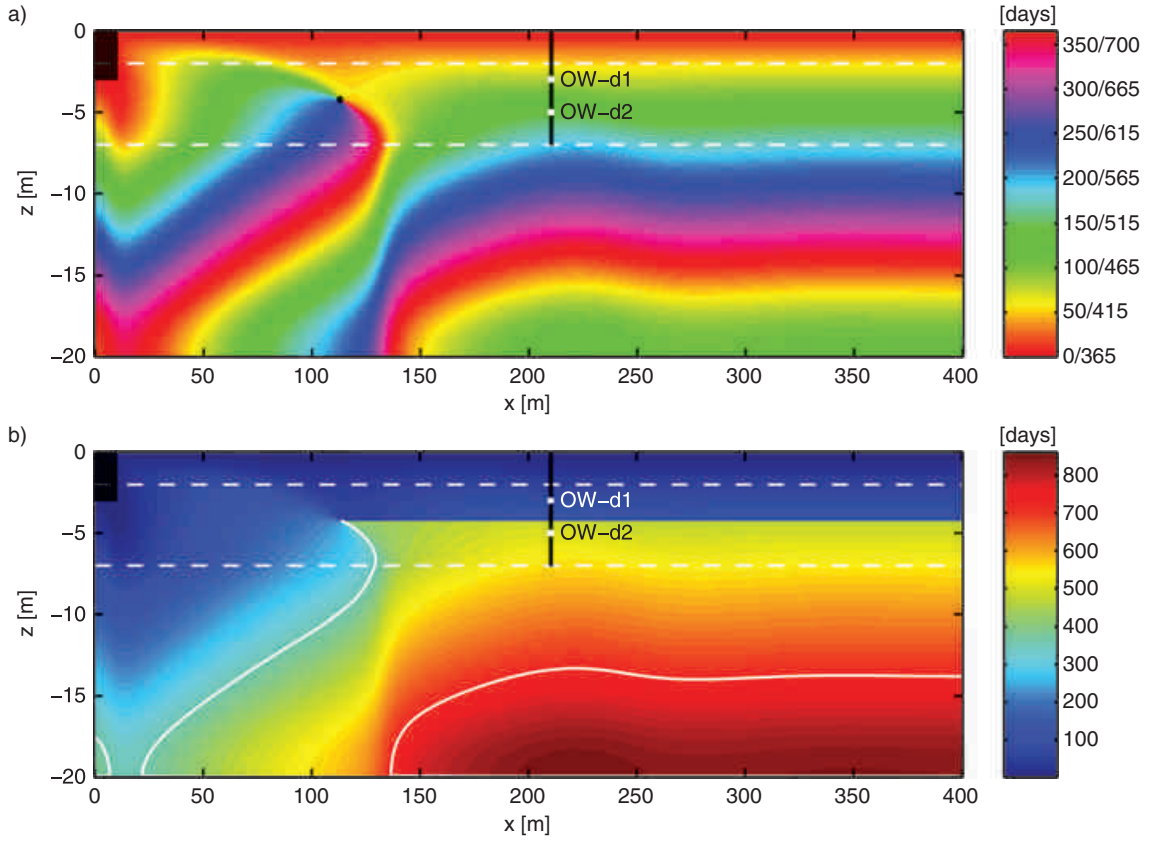

Figure 4. (a) Wrapped time shift; (b) unwrapped time shift (true isochrones). The river is located in the upper left corner. Dashed white lines: top and bottom of the aquifer; solid white lines: time shift of 1 and 2 years; black point: location where the amplitude is zero.

Sensitivity Analysis of Individual Model Elements

In the following, the full model simulation (scenario 1) is compared with predictions from simplified models (Figure 2). Results based on the RMSE as computed by Equation 27 are listed in Table 2. It should be mentioned that the calculated error introduced by simplifying surface and subsurface process simulation is sensitive to the scale of the model domain. Hence, the errors are inspected for different lengths of the model cross section.

First we discuss the results for a model length of 400 m. The value of RMSE = 0.03 K for scenario 2 is small. Considering the amplitude of 8 K, this indicates that regional groundwater recharge is only of minor importance for the simulation. This is mainly due to the low velocity of infiltration (10^{-9} m/s) compared with the average horizontal flow velocity of the aquifer (10^{-5} m/s). However, heat-transport simulation should be done with the awareness that errors could be introduced when neglecting groundwater recharge for higher recharge scenarios or during extreme hydrologic events depending on the hydrogeological setup.

Scenario 3 indicates that assuming a fully penetrating channel has a larger effect, but the RMSE is still below 1 K for a cross-section length of 400 m. Neglecting the conduction into the aquitard (scenario 4) yields a slightly higher RMSE of 1.09 K. The aquitard acts as a sink and source of heat. It stores heat during high-temperature periods and releases it during cold periods. Apparently, the aquitard needs much more attention in simulations of heat transport than in those of solute transport. This is mainly an effect of high thermal diffusion. Typical values of solute diffusion coefficients for small molecules are in the order of 10^{-9} m^2/s, whereas typical values for thermal diffusion coefficient are in the order of 10^{-7} m^2/s (Domenico and Schwartz 1998). Hence, diffusion into the underlying aquitards is of high relevance for the presented case study.

Removing the unsaturated zone (scenario 5) means that conduction into the unsaturated zone and seasonal temperature fluctuations at the land surface are ignored. This yields an error of about 1.30 K. In order to discriminate between these two factors, scenario 5 is also simulated including the unsaturated zone as the full model but without seasonal fluctuations at the surface. The result is an RMSE value of 1.0 K, and hence, the periodic boundary condition at the land surface significantly contributes to the error of scenario 5. Since the calculated errors highly depend on the chosen model geometry, general conclusions are difficult. For example, it can be expected that an increased thickness of the unsaturated zone mitigates the effect of the periodic temperature fluctuation of the top boundary on the aquifer temperature. Recall that the penetration depth for the presented model is

Table 2
RMSE of the Fourier-Transformed Temperature According to Equation 27 (K)

	Scenarios					
	2	3	4	5	6	7
Length (m)	Without Recharge	Fully Penetrating Channel	Without Aquitard	Without Unsaturated Zone	Only Aquifer	1D Analytical Solution
400	0.03	0.60	1.09	1.31	3.12	3.34
200	0.01	0.95	1.45	1.45	3.21	3.41
100	0.01	1.55	1.50	1.13	2.30	2.63
50	0.01	2.25	1.06	0.36	1.16	1.55
20	0.001	2.76	0.51	0.23	0.56	1.18

Note: Residual error of the temperature evolution in the aquifer between the full model and the simplified ones for different model lengths. Refer to Figure 2 for further details on the scenarios.

about 2 m for seasonal fluctuations and that it is controlled by flow velocity, thermal diffusivity, and the frequency.

Once more, results for scenarios 6 and 7 highlight the limited value of model conceptualizations that neglect processes such as conduction into aquitard and unsaturated zone as well as temperature fluctuations at the land surface. Applying the simplified 1D analytical equation even yields an error of 3.34 K. This is almost half of the applied amplitude of 8 K, and therefore the analytical model should be taken with caution for interpretation of seasonal temperature signals.

For shorter lengths of the model domain, the absolute errors change for each scenario, and the relative error contribution of the different model elements may vary. The shorter the model the more important the multidimensional flow component (close to the river) becomes. Shorter model domains imply a decrease of aquifer interfaces to the aquitard and unsaturated zone. Accordingly, the effects of temperature fluctuations at the surface and the conduction into the aquitard and unsaturated zone are less pronounced. For the specific conditions evaluated in this study, conduction through the top and bottom aquifer interfaces is only relevant at a distance of the observation well from the river of more than 50 m.

Figure 5 shows length profiles of the temperature amplitude and time shift averaged over the aquifer depth for the scenarios 1, 4, 5, and 7. Scenarios 2 and 3 show similar behavior to scenario 1, and scenario 6 is equivalent to scenario 7. Hence they are not shown in the figure. An extra 1D scenario which only considers convection in the aquifer is also included. Figure 5a shows the amplitude of the temperature signal as function of travel distance. After a threshold, at which the periodic signals originating from the river and the surface cancel out, the amplitude signal for scenarios 1 and 4 starts to oscillate due to the interaction between the two signals. This is in contrast to the simulations by scenarios 5 and 7, which do not account for seasonal temperature fluctuations at the surface. In these scenarios, the amplitude signal decreases exponentially with the travel distance from the river. Additionally, the amplitude signal is more dampened for scenarios 1, 4, and 5 than for scenario 7. This is attributed to the heat transfer with the underlying and overlying layers, which is simulated in scenarios 1, 4, and 5 but not in scenario 7.

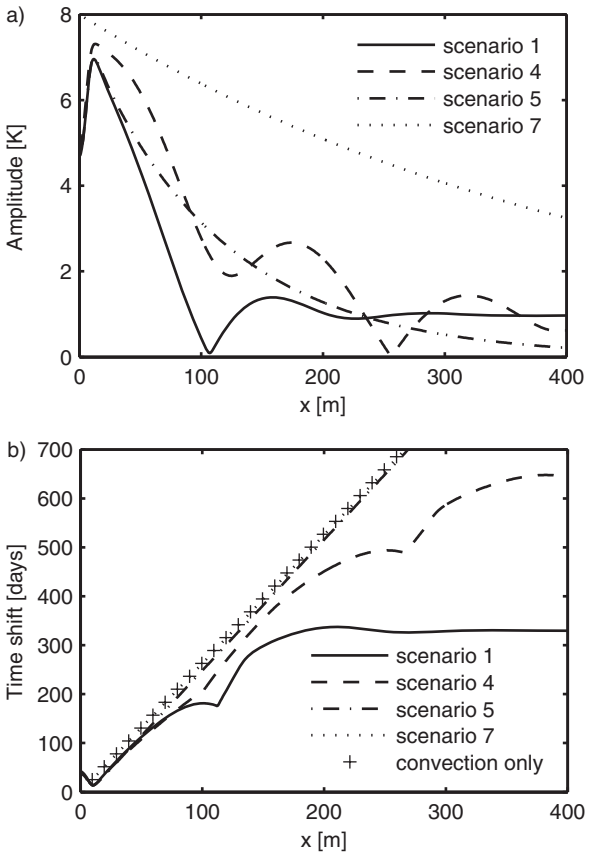

Figure 5. Longitudinal profiles of temperature amplitude (a) and time shift (b) averaged over the aquifer depth as function of distance to the river for scenarios 1 (full model), 4 (without aquitard), 5 (without unsaturated zone), and 7 (1D analytical solution) as well as an extra scenario considering only convection.

Figure 5b shows the apparent travel time of the temperature signal as a function of distance to the river. Note that an overestimation of the time shift occurs if heat exchange with the land surface is neglected. The full model (scenario 1) clearly shows that the observed time shift between the river and depth-averaged groundwater signal of temperature is dominated by exchange with the land surface at large distances. At a sufficient distance, the apparent time shift does not vary with distance anymore. Scenario 4, in which the aquitard is neglected but the unsaturated zone and land surface are accounted for, shows a similar behavior. The models neglecting the unsaturated zone, by contrast, result in a monotonic increase of time shift with distance with the exception of very close distances to the river where multi-dimensionality of the flow field is important. Assuming no influence by temperature fluctuations at the land surface results in an underestimation of the time shift of temperature signals (not shown in Figure 5) if conduction into the aquitard and unsaturated zone is neglected. This is in accordance with the fact that arrival time of the temperature front is delayed due to conduction processes into the overlying and underlying layers.

In summary, Figure 5 shows that multi-dimensionality close to the river is important at distances of up to 10 m from the bank. In the given setup, the interpretation of time shifts by essentially all models is acceptable for distances between 10 and 50 m. At larger distances, the model results start deviating. Downgradient of the point at which the two temperature signals cancel out (at about 110 m), interpretation of seasonal temperature signal by a model neglecting the heat exchange with the land surface is not possible. The exact location of this critical point depends on groundwater velocity, thickness of the unsaturated zone, and thermal conductivity. If in a field survey an almost complete disappearance of the seasonal temperature signal was observed in a dense transect of observation wells, there is only a minor chance of interpreting the reappearing seasonal signal to infiltrating river water. In practice, however, such dense transects are rare. That is, a single observation well at a distance of 150 m would exhibit a clear seasonal temperature signal with amplitude of 1 K that might be misinterpreted by mainly convective 1D transport with too high velocity.

Conclusions

We have presented a modeling study to inspect the propagation of seasonal temperature signals from an infiltrating river into an adjacent aquifer. As key measures, we have considered the amplitude and time shift of the seasonal temperature signal. In particular the latter would be used to estimate groundwater velocities from the time series. We have evaluated simplifications of physical processes in the model concept in order to assess which components of the modeled system have a major impact on the chosen measures.

In general, we can conclude that heat transfer by conduction from the aquifer into the unsaturated zone and into an underlying aquitard significantly influences the temperature signal distribution in a shallow aquifer. Arrival times of temperature signals at observation wells are underestimated when conduction into the overlying and underlying layers is neglected. The conduction into the aquitard causes additional attenuation of the seasonal temperature signal and a distinct vertical profile of the time shift. Conduction into the unsaturated zone would have identical effects if there was no influence by temperature fluctuations at the land surface. Interference of the signal originating from bank infiltration with that from the land surface leads to complex spatial patterns of amplitude and time shift, including a point at which both signals cancel out. This implies that a unique interpretation of apparent travel times from measurements of temperature time series in individual groundwater observation wells is often problematic. In the given context, a simple mismatch by multiples of 1 year may be the simplest cause of confusion, but the interference of different temperature signals can also cause noninteger offsets between simplistic 1D simulations and the full model.

In our synthetic case study, the propagation of seasonal temperature fluctuations through the aquifer was not sensitive to regional groundwater recharge. This reflects the minor impact of convective heat transfer by groundwater recharge compared to conduction through the unsaturated zone and convection within the aquifer. The relative importance of convection by groundwater recharge would increase with a larger thickness of the unsaturated zone and larger distances to the river.

Multi-dimensionality of the flow field was important only at small distances to the river. At short travel distances, time shifts between temperature time series observed on observation wells to those of the river mainly reflect convective heat transport along the curvilinear flow path from the river to the observation point. Besides the difficulty of identifying this flow path, analyzing time series from observation points close to the river suffer from the small time shift. For a seasonal signal, an offset of at least 1 month is required to obtain a reasonable estimate of apparent travel times.

The geothermal heat flux has of course no effect on seasonal fluctuations because it does not vary on a seasonal time scale. In contrast, heat conduction from the aquifer into underlying aquitard can be of high relevance. In our setup, the most simplistic models that ignore the lateral heat-flux components yield significant residual errors over larger distances, indicating that these models become invalid for interpretation of measured temperature time series. There is a certain range of distances (in our setup between $\sim$10 and 50 m) in which the time shifts computed by the various models are similar. Only within this range the simplified models would be valid for interpretation of measured temperature time series.

Most current conceptualizations for the determination of bank infiltration and travel times from time series rely on 1D analytical expressions or simplified numerical models. As pointed out, they are applicable only over a limited range of distances where assuming strictly

1D convective-dispersive heat transfer between the river and the observation well is not introducing a severe bias. This range depends on groundwater velocity, that is, the very parameter to be estimated by the analysis, on the thickness of the aquifer and that of the unsaturated zone. Our general recommendation for practical applications is to perform simulations that include conduction into the overlying and underlying layers as well as fluctuations of the land-surface temperature, such as our scenario 3, to test whether the model of an insulated 1D tube is a valid simplification for the given travel distance. If a significant bias becomes evident, the analysis of the time series requires the more complex model.

Acknowledgments

Financial support from the International Postgraduate Studies in Water Technologies (IPSWaT) by the Federal Ministry for Education and Research (BMBF) of Germany and by the ECO-GHP project funded by the EU is profoundly acknowledged. Furthermore, we would like to thank Margaret Hass for her support in the preparation of the manuscript. Last but not the least, we would like to thank, Dr. Grant Ferguson, Dr. David A. Stonestrom, and one anonymous reviewer for their constructive comments and suggestions in reviewing the manuscript.

Appendix

Spectral Representation

Usually, state variables are evaluated as function of space and time. Because we study time-periodic signals with frequency of 1/year, it is convenient to transform the governing equations into the frequency domain by Fourier transformation. The Fourier transform of the time-dependent temperature $T(t)$ is defined as (Bracewell 2000):

$$\tilde{T}(f) = \int_{-\infty}^{\infty} T(t) \exp(-2\pi i t f) \mathrm{d}t \tag{A1}$$

with the frequency f and the imaginary number $i = \sqrt{-1}$. In general, $\tilde{T}$ is a complex number. Equation A1 implies that the Fourier transform of the time derivative is as follows:

$$\frac{\partial \tilde{T}}{\partial t} = 2\pi i f \tilde{T}(f) \tag{A2}$$

Then, we can apply the Fourier transform to Equation 7 and make use of orthogonality properties, resulting in a steady-state transport equation of the Fourier-transformed temperature $\tilde{T}$, which must be met for each frequency $f (\forall f)$:

$$2\pi i f \tilde{T} + \nabla \cdot (\mathbf{v}_T \tilde{T}) - \nabla \cdot (\mathbf{D} \nabla \tilde{T}) = 0 \ \forall f \tag{A3}$$

subject to the boundary conditions:

$$\tilde{T} = \tilde{\hat{T}}_0(f) \forall f \quad \text{on } \Gamma_{\text{in}} \tag{A4}$$

$$(\mathbf{D} \nabla \tilde{T}) \cdot \boldsymbol{n} = 0 \ \forall f \quad \text{on } \frac{\Gamma}{\Gamma_{\text{in}}} \tag{A5}$$

where $\tilde{T}$ depends on frequency f and space.

We may consider the real and imaginary contributions to Equation A3 as a system of coupled equations:

$$-2\pi i f \, \mathrm{Im}(\tilde{T}) + \mathbf{v}_T \nabla \cdot [\mathrm{Re}(\tilde{T})] - \nabla \cdot [\mathbf{D} \nabla \mathrm{Re}(\tilde{T})] = 0 \ \forall f \tag{A6}$$

$$2\pi i f \, \mathrm{Re}(\tilde{T}) + \mathbf{v}_T \nabla \cdot [\mathrm{Im}(\tilde{T})] - \nabla \cdot [\mathbf{D} \nabla \mathrm{Im}(\tilde{T})] = 0 \ \forall f \tag{A7}$$

subject to:

$$\mathrm{Re}(\tilde{T}) = \mathrm{Re}(\tilde{\hat{T}}_0) \forall f \quad \text{on } \Gamma_{\text{in}} \tag{A8}$$

$$\mathrm{Im}(\tilde{T}) = \mathrm{Im}(\tilde{\hat{T}}_0) \forall f \quad \text{on } \Gamma_{\text{in}} \tag{A9}$$

$$\left[\mathbf{D} \nabla \mathrm{Re}(\tilde{T})\right] \cdot \boldsymbol{n} = 0 \ \forall f \quad \text{on } \frac{\Gamma}{\Gamma_{\text{in}}} \tag{A10}$$

$$\left[\mathbf{D} \nabla \mathrm{Im}(\tilde{T})\right] \cdot \boldsymbol{n} = 0 \ \forall f \quad \text{on } \frac{\Gamma}{\Gamma_{\text{in}}} \tag{A11}$$

Solving the convection-dispersion equation in the spectral domain provides the benefit of substituting the transient equation with a system of two steady-state equations. This can be done if a single sinusoidal signal is considered and hence $\tilde{T}$ is nonzero for only a single frequency f. In our case, this is $f = 1/\text{year}$. For a boundary condition with arbitrary inflow temperature $\hat{T}_0(t)$, however, solving the convection-dispersion equation in the spectral domain provides hardly any benefit, since the integration in time is replaced by solving the spectral equation for all frequencies.

References

Anderson, M.P. 2005. Heat as a ground water tracer. *Ground Water* 43, no. 6: 951–968.

Barlow, J.R.B., and R.H. Coupe. 2009. Use of heat to estimate streambed fluxes during extreme hydrologic events. *Water Resources Research* 45, no. 1: W01403.

Bear, J. 1972. *Dynamics of Fluids in Porous Media.* New York: American Elsevier Publishing Company Inc.

Bense, V.F., and H. Kooi. 2004. Temporal and spatial variations of shallow subsurface temperature as a record of lateral variations in groundwater flow. *Journal of Geophysical Research* 109, no. B4: B04103.

Blasch, K.W., T.P.A. Ferré, J.P. Hoffmann, and J.B. Fleming. 2006. Relative contributions of transient and steady state infiltration during ephemeral streamflow. *Water Resources Research* 42, no. 8: W08405.

Bracewell, R.N. 2000. *The Fourier Transform and Its Applications*, 3rd ed. New York: McGraw-Hill International Editions.

Bravo, H.R., F. Jiang, and R.J. Hunt. 2002. Using groundwater temperature data to constrain parameter estimation in a

groundwater flow model of a wetland system. *Water Resources Research* 38, no. 8: 1153.

Bredehoeft, J.D., and I.S. Papaopulos. 1965. Rates of vertical groundwater movement estimated from the Earth's thermal profile. *Water Resources Research* 1, no. 2: 325–328.

Brooks, A.N., and T.J.R. Hughes. 1982. Streamline upwind/Petrov-Galerkin formulations for convection dominated flows with particular emphasis on the incompressible Navier–Stokes equations. *Computer Methods in Applied Mechanics and Engineering* 32, no. 1–3: 199–259.

Bundschuh, J. 1993. Modeling annual variations of spring and groundwater temperatures associated with shallow aquifer systems. *Journal of Hydrology* 142, no. 1–4: 427–444.

Carsel, R., and R. Parrish. 1988. Developing joint probability distributions of soil water retention characteristics. *Water Resources Research* 24, no. 5: 755–769.

Cirpka, O.A., N.F. Michael, H. Markus, H. Eduard, T. Aronne, K. Rolf, and K.K. Peter. 2007. Analyzing bank filtration by deconvoluting time series of electric conductivity. *Ground Water* 45, no. 3: 318–328.

Conant, B.J. 2004. Delineating and quantifying ground water discharge zones using streambed temperatures. *Ground Water* 42, no. 2: 243–257.

Constantz, J. 2008. Heat as a tracer to determine streambed water exchanges. *Water Resources Research* 44, no. 12: W00D10.

Constantz, J. 1998. Interaction between stream temperature, streamflow, and groundwater exchanges in Alpine streams. *Water Resources Research* 34, no. 7: 1609–1616.

Constantz, J., M.H. Cox, and G.W. Su. 2003. Comparison of heat and bromide as ground water tracers near streams. *Ground Water* 41, no. 5: 647–656.

Constantz, J., A.E. Stewart, R. Niswonger, and L. Sarma. 2002. Analysis of temperature profiles for investigating stream losses beneath ephemeral channels. *Water Resources Research* 38, no. 12: 1316.

de Marsily, G. 1986. *Quantitative Hydrogeology.* San Diego, California: Academic Press.

Domenico, P.A., and F.W. Schwartz. 1998. *Physical and Chemical Hydrogeology*, 2nd ed. New York: John Wiley & Sons Inc.

Duque, C., M.L. Calvache, and P. Engesgaard. 2010. Investigating river-aquifer relations using water temperature in an anthropized environment (Motril-Salobreña aquifer). *Journal of Hydrology* 381, no. 1–2: 121–133.

Goto, S., M. Yamano, and M. Kinoshita. 2005. Thermal response of sediment with vertical fluid flow to periodic temperature variation at the surface. *Journal of Geophysical Research* 110, no. 1: B01106.

Hatch, C.E., A.T. Fisher, J.S. Revenaugh, J. Constantz, and C. Ruehl. 2006. Quantifying surface water–groundwater interactions using time series analysis of streambed thermal records: Method development. *Water Resources Research* 42, no. 10: W10410.

Healy, R.W., and A.D. Ronan. 1996. Documentation of computer program VS2DH for simulation of energy transport in variably saturated porous media. Modification of the US Geological Survey's Computer Program VS2DT. Water-Resources Investigations Report 96–4230. Denver, Colorado: USGS.

Hecht-Méndez, J., N. Molina-Giraldo, P. Blum, and P. Bayer. 2010. Evaluating MT3DMS for heat transport simulation of closed geothermal systems. *Ground Water* 48, no. 5: 741–756.

Hoehn, E., and O.A. Cirpka. 2006. Assessing residence times of hyporheic ground water in two alluvial flood plains of the Southern Alps using water temperature and tracers. *Hydrology and Earth Systems Sciences* 10, no. 4: 553–563.

Keery, J., A. Binley, N. Crook, and J.W.N. Smith. 2007. Temporal and spatial variability of groundwater-surface water fluxes: Development and application of an analytical method using temperature time series. *Journal of Hydrology* 336, no. 1–2: 1–16.

Langguth, H.-R., and R. Voigt. 2004. *Hydrogeologische Methoden.* Berlin: Springer Verlag.

Lapham, W.W. 1989. Use of temperature profiles beneath streams to determine rates of vertical ground-water flow and vertical hydraulic conductivity. Water-Supply Paper 2337. Denver, Colorado: USGS.

Ma, R., and C. Zheng. 2010. Effects of density and viscosity in modeling heat as a groundwater tracer. *Ground Water* 48, no. 3: 380–389.

Nield, D.A., and A. Bejan. 2006. *Convection in Porous Media*, 3rd ed. New York: Springer.

Niswonger, R.G., and D.E. Prudic. 2003. Modeling heat as a tracer to estimate streambed seepage and hydraulic conductivity. In *Heat as a Tool for Studying the Movement of Ground Water Near Streams*, ed. D.A. Stonestrom and J. Constantz, 81–89. USGS Circular 1260. Reston, Virginia: USGS.

Riva, M., L. Guadagnini, A. Guadagnini, T. Ptak, and E. Martac. 2006. Probabilistic study of well capture zones distribution at the Lauswiesen field site. *Journal of Contaminant Hydrology* 88, no. 1–2: 92–118.

Ronan, A.D., D.E. Prudic, C.E. Thodal, and J. Constantz. 1998. Field study and simulation of diurnal temperature effects on infiltration and variably saturated flow beneath an ephemeral stream. *Water Resources Research* 34, no. 9: 2137–2153.

Spitz, K., and J. Moreno. 1996. *A Practical Guide to Groundwater and Solute Transport Modeling.* New York: John Wiley & Sons Inc.

Stallman, R.W. 1965. Steady one-dimensional fluid flow in a semi-infinite porous medium with sinusoidal surface temperature. *Journal of Geophysical Research* 70, no. 12: 2821–2827.

Stonestrom, D.A., and K.W. Blasch. 2003. Determining temperature and thermal properties for heat-based studies of surface-water ground-water interactions. In *Heat As a Tool for Studying the Movement of Ground Water Near Streams*, ed. D.A. Stonestrom and J. Constantz, 73–80. USGS Circular 1260. Reston, Virginia: USGS.

Su, G.W., J. Jasperse, D. Seymour, and J. Constantz. 2004. Estimation of hydraulic conductivity in an alluvial system using temperatures. *Ground Water* 42, no. 6: 890–901.

Suzuki, S. 1960. Percolation measurements based on heat flow through soil with special reference to paddy fields. *Journal Geophysical Research* 65, no. 9: 2883–2885.

Taniguchi, M. 1993. Evaluation of vertical groundwater fluxes and thermal properties of aquifers based on transient temperature-depth profiles. *Water Resources Research* 29, no. 7: 2021–2026.

van Genuchten, M.T. 1980. A closed-form equation for predicting the hydraulic conductivity of unsaturated soils. *Soil Science Society of America Journal* 44, no. 5: 892–898.

Vogt, T., P. Schneider, L. Hahn-Woernle, and O.A. Cirpka. 2010. Estimation of seepage rates in a losing stream by means of fiber-optic high-resolution vertical temperature profiling. *Journal of Hydrology* 380, no. 1–2: 154–164.

Voss, C.I. 1984. SUTRA: A finite element simulation model for saturated–unsaturated, fluid-density-dependent groundwater flow energy transport or chemical-reactive single-species solute transport. Water-Resources Investigations Report 84–4369. Reston, Virginia: USGS.

Woessner, W.W. 2000. Stream and fluvial plain ground water interactions: Rescaling hydrogeologic thought. *Ground Water* 38, no. 3: 423–429.